Oncogene (2006) 25, 2860–2872
© 2006 Nature Publishing Group All rights reserved 0950-9232/06 $30.00
www.nature.com/onc

ORIGINAL ARTICLE

Fhit modulation of the Akt-survivin pathway in lung cancer cells: Fhit-tyrosine 114 (Y114) is essential

S Semba[1], F Trapasso[1,2], M Fabbri[1], KA McCorkell[1], S Volinia[1,3], T Druck[1], D Iliopoulos[1], Y Pekarsky[1], H Ishii[4], PN Garrison[5], LD Barnes[5], CM Croce[1] and K Huebner[1]

[1]Comprehensive Cancer Center and Department of Molecular Virology, Immunology, and Medical Genetics, The Ohio State University, Columbus, OH, USA; [2]Department of Experimental and Clinical Medicine, Medical School of Catanzaro, 'Magna Graecia' University of Catanzaro, Catanzaro, Italy; [3]Telethon Facility-Data Mining for Analysis of DNA Microarrays, Università degli Studi, Ferrara, Italy; [4]Division of Stem Cell Regulation/Molecular Hematopoiesis, Center for Molecular Medicine, Jichi Medical School, Minami-Kawachi, Japan and [5]Department of Biochemistry, University of Texas Health Science Center, San Antonio, TX, USA

The Fhit tumor suppressor binds and hydrolyses diadenosine polyphosphates and the Fhit–substrate complex has been proposed as a proapoptotic effector, as determined by infection of susceptible cancer cells with adenoviruses carrying wild-type *fragile histidine triad (FHIT)* or catalytic site mutants. The highly conserved Fhit tyrosine 114 (Y114), within the unstructured loop C-terminal of the catalytic site, can be phosphorylated by Src family tyrosine kinases, although endogenous phospho-Fhit is rarely detected. To explore the importance of Y114 and identify Fhit-mediated signaling events, wild-type and Y114 mutant *FHIT*-expressing adenoviruses were introduced into two human lung cancer cell lines. Caspase-dependent apoptosis was effectively induced only by wild-type but not Y114 mutant Fhit proteins. By expression profiling of *FHIT* versus mutant *FHIT*-infected cells, we found that *survivin*, an Inhibitor of Apoptosis Protein (IAP) family member, was significantly decreased by wild-type Fhit. In addition, Fhit inhibited activity of Akt, a key effector in the phosphatidylinositol 3-OH kinase (PI3K) pathway; loss of endogenous Fhit expression caused increased Akt activity *in vitro* and *in vivo*, and overexpression of constitutively active Akt inhibited Fhit-induced apoptosis. The results indicate that the Fhit Y114 residue plays a critical role in Fhit-induced apoptosis, occurring through inactivation of the PI3K-Akt-survivin signal pathway.
Oncogene (2006) **25,** 2860–2872. doi:10.1038/sj.onc.1209323; published online 16 January 2006

Keywords: Fhit; tyrosine 114 (Y114); Akt; survivin; lung cancer; apoptosis

Correspondence: Dr K Huebner, Comprehensive Cancer Center and Department of Molecular Virology, Immunology, and Medical Genetics, The Ohio State University, Room 455C Wiseman Hall, 410 West 12th Avenue, Columbus, OH 43210, USA.
E-mail: kay.huebner@osumc.edu
Received 22 July 2005; revised 17 October 2005; accepted 14 November 2005; published online 16 January 2006

Introduction

The *fragile histidine triad (FHIT)* gene spans the most active common fragile site in the human genome, *FRA3B* (3p14.2), which is frequently involved in biallelic loss, genomic rearrangement and cytogenetic abnormalities in tumors (Ohta *et al*., 1996; Sozzi *et al*., 1996; Huebner *et al*., 1998). Although somatic mutation within the *FHIT* gene is rare, deletions at the *FHIT* locus, abnormal *FHIT* transcripts, promoter hypermethylation and loss of Fhit expression were frequently detected in human malignancies, including those of the lung, head and neck, esophagus, stomach, breast and bladder (Huebner *et al*., 1998; Croce *et al*., 1999; Kuroki *et al*., 2003; Iliopoulos *et al*., 2005). Loss of Fhit expression is observed not only in cancers but also in premalignant lesions, confirming that the *FHIT* gene is susceptible to damage caused by environmental carcinogens in initial steps of multistep carcinogenesis (Huebner and Croce, 2003).

Overexpression of *FHIT* by the adenoviral gene delivery system in human cancer cells effectively suppressed cell growth and induced caspase-dependent apoptosis in *in vitro* and *in vivo* experiments (Dumon *et al*., 2001a; Ishii *et al*., 2001; Roz *et al*., 2002; Sevignani *et al*., 2003). $Fhit^{-/-}$ and $Fhit^{+/-}$ mice exhibit increased susceptibility to spontaneous tumors and deletion of a *Fhit* allele in mice enhanced sensitivity to the carcinogen, *N*-nitrosomethylbenzylamine (NMBA); around 80% of $Fhit^{-/-}$ and $Fhit^{+/-}$ mice developed forestomach tumors (adenomas, papillomas and invasive carcinomas) after one dose of NMBA, compared with fewer than 8% in wild-type mice (Zanesi *et al*., 2001; Fujishita *et al*., 2004). Moreover, deficiency of Fhit protein altered sensitivity to mitomycin C, UVC and ionizing radiation in human gastric carcinoma cells, as well as mouse normal kidney cells, in clonogenic assays (Ottey *et al*., 2004; Hu *et al*., 2005). Thus, Fhit plays an important role in tumorigenesis, and *FHIT* gene therapy is expected to be a novel clinical approach in treatment of human cancers and prevention of tumor development (Dumon *et al*., 2001b). However, the mechanism through which Fhit induces apoptosis in cancer cells requires further elucidation.

Fhit is a member of the histidine triad (HIT) nucleotide-binding protein superfamily, encoding a diadenosine polyphosphate (Ap_nA) hydrolase that cleaves substrates such as diadenosine triphosphate (Ap_3A) and diadenosine tetraphosphate (Ap_4A) to AMP plus the other nucleotide (Barnes *et al*., 1996; Huebner *et al*., 1998). Structural studies have shown that Fhit is a dimer that binds two Ap_3A substrates, presenting a highly phosphorylated surface, with five phosphate groups and two adenosine moieties (Pace *et al*., 1998). The conserved HIT motif (His-X-His-X-His-X-X, where X is a hydrophobic residue) of Fhit is located near its C-terminal end and the hydrolytic activity of Fhit is lost when histidine 96 (H96) is replaced with asparagine (Fhit-H96N), showing that the H96 central histidine residue of the triad is essential for Ap_3A hydrolase activity (Barnes *et al*., 1996). However, Fhit Ap_3A hydrolase activity was not required for its tumor suppressor activity because Fhit-H96N, a hydrolase 'dead' mutant, also suppressed tumorigenicity *in vivo* (Siprashvili *et al*., 1997). Trapasso *et al*. (2003) tested the biochemical characteristics and biological effects of a series of mutant Fhit proteins that were intended to reduce the substrate-binding and/or hydrolytic rates; Fhit-induced apoptosis in cancer cells was correlated with the apparent substrate-binding activity (K_m) but not the substrate hydrolytic activity (k_{cat}).

Recently, it was observed that the sequence $DSIY^{114}EEL$ of Fhit, which fits the consensus for targets of phosphorylation by Src tyrosine kinase family members, could be phosphorylated *in vitro* and *in vivo* (Pekarsky *et al*., 2004). Garrison *et al*. (2005) determined the steady-state K_m and k_{cat} values for the Ap_3A hydrolase activity of recombinant unphospho-Fhit, monophospho-Fhit and diphospho-Fhit, and found that the K_m and k_{cat} values for monophospho-Fhit and diphosho-Fhit are lower than for unphospho-Fhit. If Fhit proapoptotic activity is determined mainly or solely by binding of substrate, that is by low K_m, then phosphorylation of tyrosine 114 (Y114) might be important in determining proapoptotic activity.

In this study, we constructed a series of adenoviral vectors that deliver wild-type and Y114 mutant *FHIT* genes to examine the biological relevance of the Y114 residue to proapoptosis; we found that the Fhit Y114 residue is essential for Fhit-induced apoptosis in human lung cancer cells. Microarray analysis was performed to identify genes differentially expressed in cells overexpressing wild-type and Y114 mutant Fhit. Our results identified a pathway through which Fhit induces caspase-dependent apoptosis, by inactivation of phosphatidylinositol 3-OH kinase (PI3K)-Akt-survivin signals.

Results

Fhit Y114 is required for induction of caspase-dependent apoptosis

The Y114 mutants have K_m values 5 (Fhit-Y114F), 10 (Fhit-Δ113–117) and 23 (Fhit-Y114A) times larger than wild-type Fhit and k_{cat} values that are about the same (Fhit-Y114F, Fhit-Y114A) to 42 (Fhit-Δ113–117) times lower than wild type (PN Garrison and LD Barnes, unpublished data). For analysis of the biological effects of recombinant Fhit proteins, we infected two previously investigated human lung cancer cell lines, H1299 and A549 (Ji *et al*., 1999; Trapasso *et al*., 2003). Cells were infected with adenoviruses carrying wild-type (Ad-*FHIT*-wt) and mutant *FHIT* (Ad-*FHIT*-Y114A, Ad-*FHIT*-Y114D, Ad-*FHIT*-Y114F, Ad-*FHIT*-Δ113–117) and exhibited >95% GFP-positive cells 24 h after infection. Although Fhit antiserum recognized purified recombinant phospho-Fhit protein as well as unphosphorylated forms (Figure 1A(a)), upshifted bands representing phospho-Fhit (Pekarsky *et al*., 2004; Garrison *et al*., 2005) were not detected in Ad-*FHIT*-infected cells with Fhit and phospho-Fhit antisera (data not shown). Among recombinant wild-type and the Y114 mutant Fhit proteins, there were slight differences in gel mobility; Y114 substituted with alanine (Y114A) and aspartic acid (Y114D) showed lower gel mobility but replacement with phenylalanine (Y114F) and the 113–117 deletion mutant (Δ113–117) exhibited high mobility shifts (Figure 1A(b)). All Fhit-expressing cells, whether expressing wild-type Fhit or Y114 mutants, exhibited similar levels of Fhit protein mainly in the cytoplasm, with apparent partial localization in the mitochondria (data not shown), in both H1299 and A549 cells. Representative immunofluorescence results for H1299 cells infected with Ad-*FHIT*-wt and Ad-*FHIT*-Y114F are shown in Figure 1B.

Next, we performed cell viability tests to determine the biological effect of *FHIT* recombinant adenoviruses in human lung cancer cells. Although Ad-*FHIT*-wt effectively suppressed cell growth and viability in a multiplicity of infection (MOI)-dependent manner, the Y114 mutant viruses, irrespective of whether they had single amino-acid replacement or deletion, did not show a significant growth-inhibitory effect (Supplementary Figure S1). Indeed, nearly 50% of the Ad-*FHIT*-wt-infected cells showed loss of viability 5 days after infection at MOI 25; the mutant *FHIT*-expressing viruses did not alter cell viability at MOI 25 (Figure 1C).

High levels of Adeno-transduced Fhit expression cause caspase-dependent apoptosis in cancer cells and loss of the apoptosis-inducing effect of Fhit is considered to be limited by its apparent substrate-binding activity (Trapasso *et al*., 2003). Thus, we examined the biological effect of this series of Y114 mutant *FHIT* adenoviruses that showed varying K_m values. Both H1299 and A549 cells, when infected with Ad-*FHIT*-wt, exhibited a dramatic appearance of cells with subG1 DNA content at 5 days after infection; however, the effects of recombinant mutant viruses were similar to that of the Ad-*GFP* control (Figure 2a). Levels of procaspase-3, procaspase-8 and PARP were significantly decreased only in cells infected with Ad-*FHIT*-wt and not in cells infected with mutant *FHIT* viruses (Figure 2b). We confirmed activation of caspase-dependent apoptotic signaling in Ad-*FHIT*-wt-infected cells by assessing the population of cleaved caspase-3-

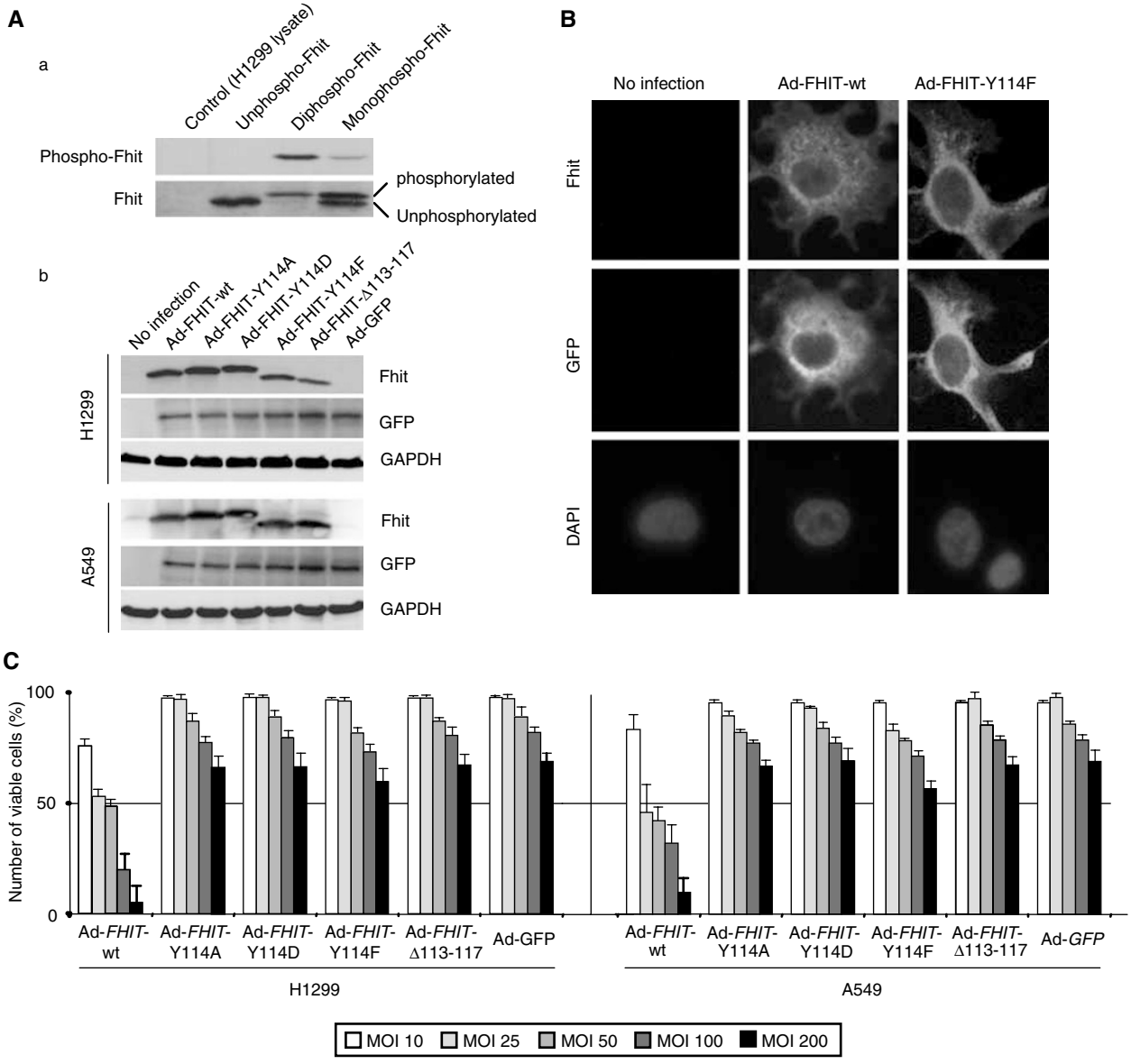

Figure 1 Characterization of wild-type and Y114 mutant *FHIT*-infected human lung cancer cells. (**A**) Detection of recombinant Fhit proteins by Western blot analysis. (**a**) Purified recombinant Fhit proteins, unphosphorylated, monophosphorylated and diphosphorylated, were detected using phospho-Fhit antiserum (upper panel) or Fhit polyclonal antiserum (lower panel); note that anti-Fhit serum detects both unphosphorylated and phosphorylated monomers. (**b**) Western blot of wild-type and mutant Fhit protein overexpressed in H1299 and A549 cells. Cells were infected with individual viruses (MOI 25) and incubated for 48 h. Individual recombinant Fhit proteins showed different gel mobilities, partially based on charge differences. Note that there was no signal indicating phospho-Fhit expression in Ad-*FHIT*-wt-infected cells. GFP and GAPDH expression levels served as loading controls. (**B**) Intracellular localization of recombinant wild-type Fhit and Fhit-Y114F proteins overexpressed in H1299 cells. The cells were infected with Ad-*FHIT*-wt and Ad-*FHIT*-Y114F, respectively (MOI 25). After 48 h, wild-type and mutant Fhit protein were detected by anti-Fhit primary antiserum followed by anti-rabbit IgG labeled with Texas-Red. DAPI-stained cells are shown for identification of nuclei. (**C**) Results of cell viability analysis in recombinant *FHIT*-infected-lung cancer cells. Five days after infection with individual viruses (MOI 25), cells were stained with trypan blue and counted. The percentage of viable cells is shown for each virus for both H1299 and A549 cell lines.

positive cells (Figure 2a). We also attempted to detect caspase-9 status in both H1299 and A549 cells, but neither of the cell lines expressed caspase-9 (data not shown), suggesting existence of other mechanism(s) of activation of executioner caspases in the Fhit-induced apoptosis pathway.

The wild-type and Y114A and Y114F mutant *FHIT* viruses were also used to infect a panel of esophageal cancer cell lines, that had been studied previously for effect of Ad-*FHIT*-wt virus (Ishii *et al*., 2001). Infection with wild-type *FHIT* virus caused apoptosis in two esophageal cancer cell lines but the Y114 mutant viruses

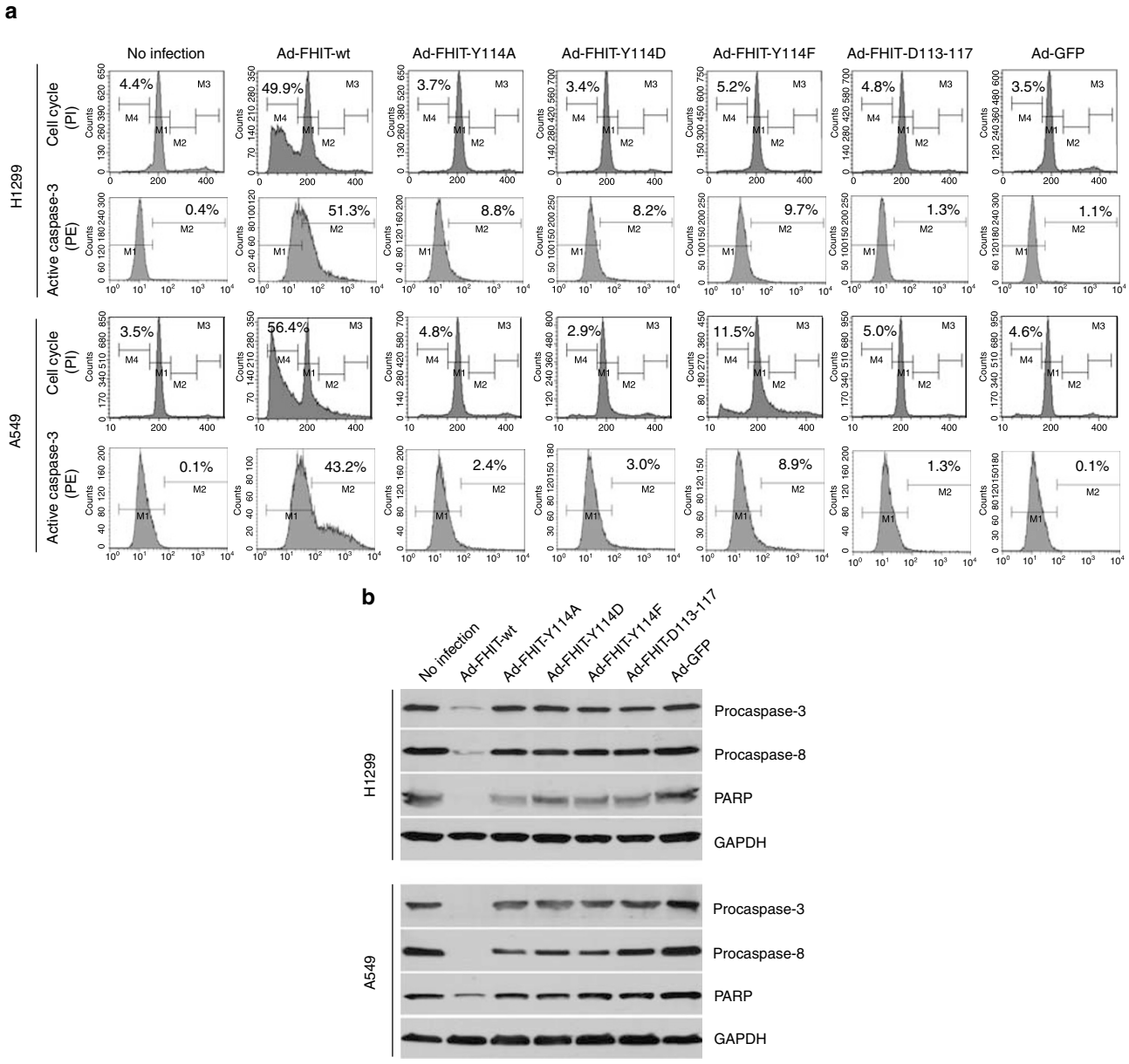

Figure 2 Caspase-dependent apoptosis induced only by Ad-*FHIT*-wt virus. (**a**) SubG1 DNA content and fraction of active caspase-3-positive cells for wild-type and mutant *FHIT*-infected human lung cancer cell lines. Flow cytometric analysis of H1299 and A549 cells infected with wild-type and mutant *FHIT* (MOI 25) was performed 5 days after viral inoculation. For subG1 DNA content analysis, the cells were stained with PI. Percent of cells in subG1 is shown in the upper left corner of each fluorogram. Anti-active (cleaved) caspase-3 mouse monoclonal antibody conjugated with PE was used to detect fractions of cells expressing cleaved caspase-3; percent of active caspase-3 expressing cells is shown in upper right corner of fluorograms. (**b**) Western blot analysis of the levels of caspase-3, caspase-8 and PARP expression in H1299 and A549 human lung cancer cells. Cells were infected with wild-type and mutant recombinant *FHIT* viruses (MOI 25) and maintained for 5 days. Note that only Ad-*FHIT*-wt decreased the levels of procaspase and non-cleaved PARP expression.

did not, in accord with the effects of these viruses on the two lung cancer cell lines (data not shown).

Expression of survivin is downregulated after wild-type Fhit expression

To identify pathways through which Fhit induces caspase-dependent cell death, we exploited the differences in the apoptosis-inducing effects among wild-type and mutant *FHIT* adenoviruses. RNAs derived from H1299 cells infected with Ad-*FHIT*-wt and Ad-*FHIT*-Y114F were used for gene expression profiling experiments. To avoid contamination with apoptotic cells, the H1299 cells infected with Ad-*FHIT* viruses were collected after 48 and 72 h. With the GeneChip Human genome U133A plus 2.0 array, the change in the gene expression profile of the H1299 cells infected with Ad-*FHIT*-wt compared with the cells infected with

Ad-*FHIT*-Y114F did not involve a large number of genes. After normalization of raw data, 22 genes were determined to have statistically significant changes in H1299 cells infected with Ad-*FHIT*-wt at both 48 and 72 h after infection (Table 1). The accuracy of the microarray analysis was confirmed by real-time RT–PCR analysis of expression of six differentially expressed genes, *heat shock 60 kDa protein 1* (*HSPD1*), *interferon-induced protein 44-like* (*IFI44L*), *2′,5′-oligoadenylate synthase 1* (*OAS1*), *junction-mediating and regulatory protein* (*JMY*), *baculoviral Inhibitor of Apoptosis Protein* (*IAP*) *repeat-containing 5*/*survivin* (*BIRC5*) and *epithelial cell transforming sequence 2 oncogene* (*ECT2*) (see Supplementary Figure S2). The results showed good concordance with the microarray data in terms of fold change of gene expression. Among the genes upregulated and downregulated by Ad-*FHIT*-wt, *survivin* showed two and sixfold downregulation, by real-time RT–PCR analysis, at 48 and 72 h after viral infection (Supplementary Figure S2). Survivin binds specifically to terminal effector cell death proteases, substantially reduces caspase activity and inhibits apoptosis in cells exposed to diverse apoptosis-triggering stimuli (Ambrosini *et al*., 1997; Li *et al*., 1998); hence, in the H1299 cells infected with Ad-*FHIT*-wt, overexpressed Fhit may contribute to *survivin* downregulation, resulting in caspase-3-mediated cell death. Time course analyses showed that the mRNA and protein levels of *survivin* expression were significantly suppressed in cells infected with Ad-*FHIT*-wt (Figure 3).

Fhit proapoptosis and the PI3K-Akt-survivin pathway

Akt, a cell survival factor and downstream target of PI3K, upregulates forkhead transcription factor activity, resulting in upregulation of a series of antiapoptotic proteins, including survivin (Mitsiades *et al*., 2002). Indeed, reduced levels of survivin protein expression were detected in the H1299 cells treated with LY294002 PI3K inhibitor (Figure 3b). To investigate the possibility that PI3K-Akt-survivin signaling is affected by Fhit overexpression, phospho-Akt expression was examined in H1299 cells infected with Ad-*FHIT*-wt; expression of phospho-Akt was suppressed by wild-type Fhit overexpression, whereas this activated form of Akt remained relatively steady in cells infected with Ad-*FHIT*-Y114F (Figure 4A). Decreased levels of phospho-Src were not detected in cells infected with Ad-*FHIT*-Y114F and wild-type *FHIT* infected cells showed reduced phospho-Src only at 5 days post infection when most cells are in various stages of apoptosis (Figure 4A), indicating that Fhit expression does not downmodulate Src activity. Also, we confirmed that the level of phospho-mTOR, a downstream target of Akt, was suppressed by wild-type Fhit (Figure 4A). Ad-*GFP* infection did not alter the

Table 1 Genes differentially expressed in H1299 cells infected with Ad-*FHIT*-wt compared with Ad-*FHIT*-Y114F: SAM paired data comparison

Accession number	*Gene title*	*Symbol*	*Fold change*	*Molecular function/biological process*
Upregulated genes				
NM_002156	Heat shock 60 kDa protein 1	HSPD1	16.632	ATP binding/mitochondrial matrix protein import
NM_006820	Interferon-induced protein 44-like	IFI44L	10.346	—
NM_032888	Collagen, type XXVII, α1	COL27A1	9.308	Extracellular matrix structural consituent/ cell adhesion
NM_181291	WD repeat domain 20	WDR 20	9.297	—
NM_016816	2′,5′-oligoadenylate synthase 1	OAS1	8.971	ATP binding/immune response
AF086061	Fibroblast growth factor receptor substrate 2	FRS2	6.917	Insulin receptor binding/G-protein coupled receptor signaling
NM_000332	Ataxin 1	ATXN1	6.358	RNA binding
NM_025217	UL16 binding protein 2	ULBP2	5.621	MHC class I receptor activity/antigen presentation
NM_000088	Collagen, type I, α1	COL1A1	5.271	Extracellular matrix structural constituent
NM_015364	Lymphocyte antigen 96	LY96	4.307	Coreceptor activity/antibacterial humoral response
NM_152405	Junction-mediating and regulatory protein	JMY	4.232	—
NM_182965	Sphingosine kinase 1	SPHK1	3.486	D-erythrosphingosine kinase activity
Downregulated genes				
NM_016343	Centromere protein E, 312 kDa	CENPE	0.052	ATP binding/DNA replication and chromosomal cycle
NM_018136	Abnormal spindle-like microcephaly associated	ASPM	0.175	Calmodulin binding/mitosis
NM_018365	Meiosis-specific neural structural protein 1	MNS1	0.207	—
NM_006461	Sperm associated antigen 5	SPAG5	0.208	Cell cycle
NM_001168	Baculoviral IAP repeat-containing 5 (survivin)	BIRC5	0.215	Caspase inhibitor activity/G_2/M transition of mitotic cell cycle
NM_014264	Polo-like kinase 4	PLK4	0.353	ATP binding/protein amino-acid phosphorylation
NM_012145	Deoxythymidylate kinase	DTYMK	0.407	ATP binding/DNA metabolism
BC019922	Zinc finger protein 252	ZNF252	0.407	Nucleic acid binding
NM_018098	Epithelial cell transforming sequence 2 oncogene	ECT2	0.481	Guanyl-nucleotide exchange factor activity
NM_017882	Ceroi-lipofuscinosis, neuronal 6, variant	CLN6	0.515	—

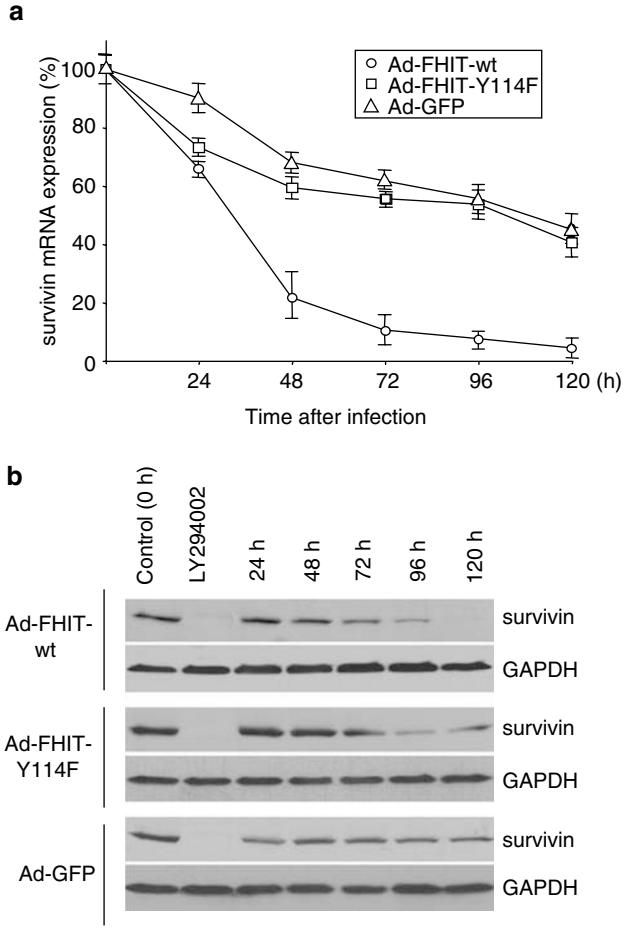

Figure 3 Effect of Fhit expression on *survivin* mRNA and protein expression in H1299 cells. (**a**) Results of quantitative real-time RT–PCR analysis of *survivin* mRNA expression. The levels of *survivin* mRNA expression before infection with adenoviruses are considered to be 100%. The cells were infected with Ad-*FHIT*-wt, Ad-*FHIT*-Y114F and Ad-*GFP*, respectively (MOI 25), and total RNAs isolated from these cells were used. Expression levels of *survivin* mRNA were calculated according to the $2^{-\Delta\Delta Ct}$ method, as described in the text. (**b**) Western blot analysis of altered levels of survivin protein. Adenoviruses were inoculated at an MOI of 25. Cells were also treated with LY294002, a PI3K inhibitor (20 μM) for 24 h. Note that expression of survivin was effectively suppressed by LY294002, illustrating that the PI3K pathway controls survivin expression. GAPDH served as protein loading control.

levels of phosphorylated forms of Akt, Src and mTOR (data not shown).

To determine whether suppression of endogenously expressed Fhit could upregulate Akt activity, A549 cells, expressing a low level of endogenous Fhit, were transfected with *FHIT* small interfering RNA (siRNA) (Figure 4B(a)). Suppression of endogenous Fhit expression by *FHIT* siRNA increased phospho-Akt levels to a maximum at 48 h (Figure 4B(b)). *FHIT*-specific and scrambled *FHIT* siRNAs did not affect *GAPDH* mRNA expression (Figure 4B(b)), and neither expression of Fhit nor Akt were altered by *GAPDH* siRNA transfection (data not shown). To examine the possibility that loss of Fhit expression can activate PI3K-Akt-survivin signaling *in vivo*, we also investigated the levels of phospho-Akt and survivin expression in wild-type and Fhit-deficient mouse tissues immunohistochemically. In normal bronchial epithelial cells of wild-type mice with abundant Fhit expression, phospho-Akt and survivin expression were not detected immunohistochemically (Figure 4C(a, b, c)). However, in normal lung tissue sections from Fhit$^{-/-}$ mice, the basal level of phospho-Akt expression was slightly increased, along with higher levels of survivin than in normal bronchial epithelium of a wild-type mouse (Figure 4C(d, e, f). Interestingly, Fhit-deficient mouse lung tumors demonstrated strong phospho-Akt and survivin expression compared with both wild-type and Fhit$^{-/-}$ mouse normal tissues (Figure 4C(g, h, i)).

Constitutively active Akt inhibits Fhit-induced apoptosis

To investigate the influence of Akt on Fhit proapoptotic function, we established H1299 and A549 cells expressing constitutively active Akt. After infection with Ad-*FHIT*-wt, the cellular fractions with subG1 DNA content were significantly decreased relative to control cells (Figure 5a). Simultaneously, the fractions of caspase-3-positive cells were decreased by 21.3 and 39.8% in H1299 and A549 cells, respectively; however, activated Akt did not completely inhibit the induction of caspase-dependent apoptosis (Figure 5b). We confirmed the protein levels of phospho-Akt and survivin, as well as caspases. Constitutively active Akt indeed upregulated basal levels of survivin and caspase family members compared with control cells (Figure 5c). Although this Akt-survivin-mediated apoptosis was induced by Ad-*FHIT*-wt infection in control cells, overexpression of activated Akt inhibited the effects of Fhit in downregulation of survivin expression and subsequent activation of caspases (Figure 5c).

Discussion

Fhit is a small (16.8 kDa) protein that is highly conserved from fungi to man (~60% similar in *Schizosaccharomyces pombe* and *Homo sapiens*). Fhit protein is likely to have multiple, probably interrelated, functions: (1) influencing the DNA-damage response to mitomycin C, UVC and ionizing radiation (Ottey *et al*., 2004; Hu *et al*., 2005); (2) in suppression of growth of tumors after Fhit replacement (Croce *et al*., 1999; Zanesi *et al*., 2001); (3) as a proapoptotic signal protein when overexpressed in Fhit-deficient cancer cells (Ji *et al*., 1999; Dumon *et al*., 2001a; Ishii *et al*., 2001; Roz *et al*., 2002). Among these functions, Fhit proapoptotic signaling is perhaps the pathway most amenable to mechanistic analysis, and in this study we have been able to identify several downstream effectors of the apoptotic pathway and determine that mutation of the Fhit Y114 residue, highly conserved and susceptible to phosphorylation *in vivo* and *in vitro*, abrogates the proapoptotic function of Fhit. We had previously shown that kinetic features of the Fhit-substrate interaction were highly

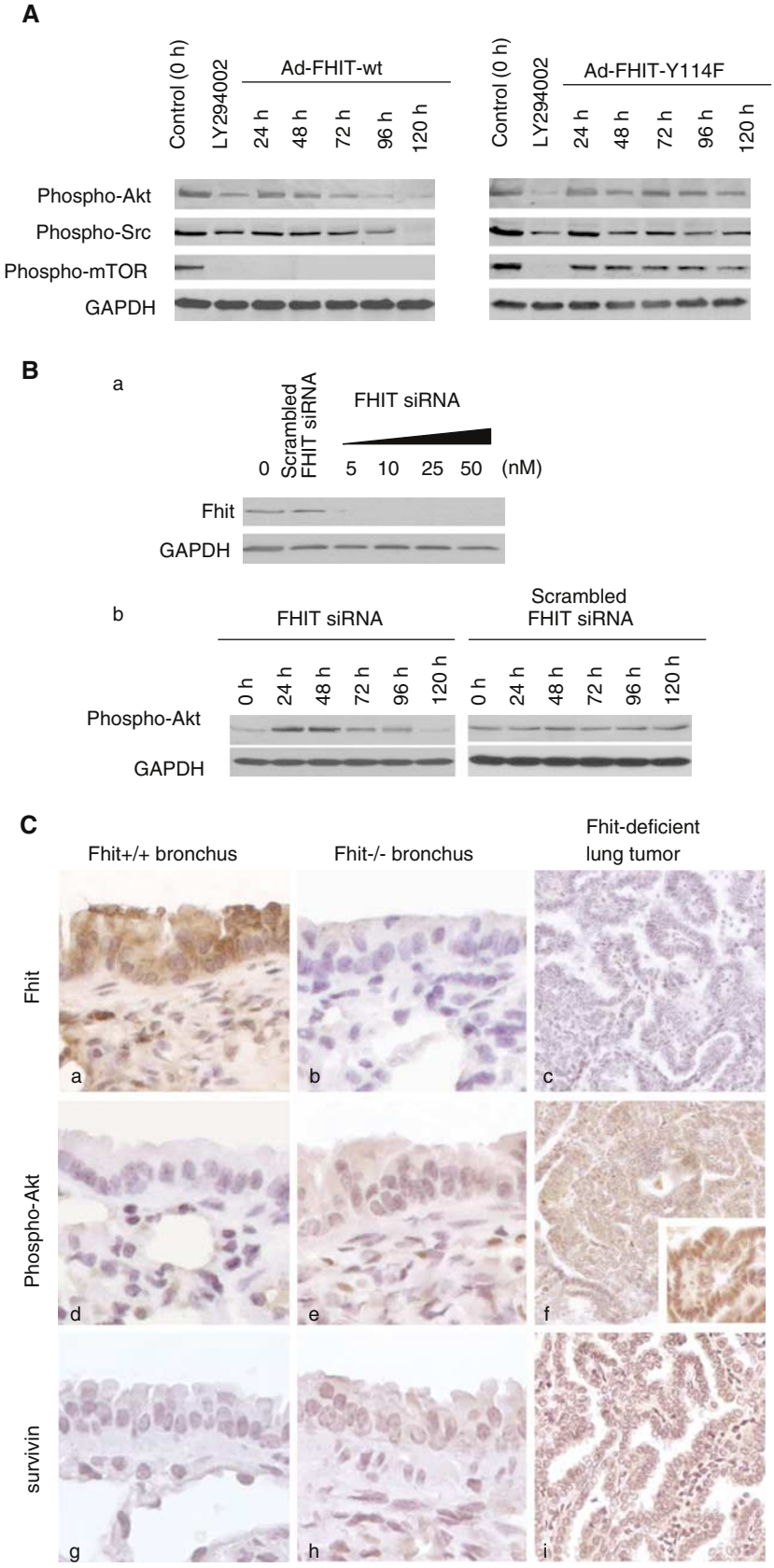
A
Control (0 h)
LY294002
Ad-FHIT-wt
24 h
48 h
72 h
96 h
120 h
Control (0 h)
LY294002
Ad-FHIT-Y114F
24 h
48 h
72 h
96 h
120 h
Phospho-Akt
Phospho-Src
Phospho-mTOR
GAPDH
B
a
Scrambled FHIT siRNA
FHIT siRNA
0
5
10
25
50
(nM)
Fhit
GAPDH
b
FHIT siRNA
Scrambled FHIT siRNA
0 h
24 h
48 h
72 h
96 h
120 h
0 h
24 h
48 h
72 h
96 h
120 h
Phospho-Akt
GAPDH
C
Fhit+/+ bronchus
Fhit-/- bronchus
Fhit-deficient lung tumor
Fhit
Phospho-Akt
survivin
a
b
c
d
e
f
g
h
i

relevant to proapoptotic function, with mutations that increase $K_{m,}$ rather than k_{cat}, causing loss of proapoptosis; that is, Fhit proteins that apparently bind substrate well, even if lacking catalytic function, were the best apoptosis inducers (Siprashvili *et al*., 1997; Trapasso *et al*., 2003). Now a series of Fhit Y114 mutants, with varying K_m and k_{cat} values, has been tested for proapoptotic function. The highly conserved (from *S. pombe* to *H. sapiens*) tyrosine at position 114 of human Fhit is within an unstructured 20 amino-acid loop that has been invisible in all reported Fhit structures (Pace *et al*., 1998). Preliminary X-ray crystallographic studies show that the loop is less flexible (i.e., more visible) when Y114 is phosphorylated (H Pace and LD Barnes, unpublished data) and we hypothesize that the loop in phosphorylated forms may hover over the substrate surface, simultaneously allowing lowered K_m values but possibly obscuring the Fhit–substrate signaling surface.

The biological effects of the series of recombinant adenoviral vectors analysed in this study were compatible with the data on their substrate-binding activity; that is, Y114 mutant Fhit proteins had higher K_m's and were less capable of inducing caspase-dependent apoptosis in human lung cancers. How does the single amino-acid substitution at Y114 diminish the apparent substrate-binding activity? Fhit-Y114F, structurally and kinetically most similar to wild-type Fhit, consistently exhibited some minor apoptotic function. Fhit-Y114D was designed to mimic the negative charge of a phosphorylated Y114, and indeed the aspartic acid substitution of Fhit-Y114D is upshifted to the same position as a denatured phospho-Fhit monomer on SDS–PAGE gel. However, the Fhit-Y114D mutant did not induce apoptosis, possibly because replacement with aspartic acid does not mimic the phosphorylated Y114. It is also possible that Y114D does mimic the phosporylated form, thereby inactivating Fhit apoptotic function and contradicting our hypothesis that Fhit phosphorylation may enhance Fhit apoptotic function. Although the K_m value for Y114D was not determined, these data suggest that Fhit-Y114D may have a high K_m value. Neither Fhit-Y114A nor Fhit-Δ113–117, expected to alter the structure in the unstructured loop near the Fhit catalytic site, had tumor suppressor activity, which was compatible with their apparent low affinities for substrate. Taken together, these findings suggest that the Y114 residue, within an invisible loop in all crystal structures, including those with bound substrate analog, plays a critical role in stability of the Fhit–Ap_3A complex, the proposed active, tumor-suppressing form of Fhit. The biological significance of phosphorylation of Fhit at codon 114 was not significantly clarified by these studies. The low K_m values for purified monophospho-Fhit (0.67 μM) and diphospho-Fhit (0.66 μM) suggested the possibility of higher tumor suppressor activity of phosphorylated forms of Fhit than unphospho-Fhit (Garrison *et al*., 2005). Although we attempted to detect phosphorylated forms of Fhit with Fhit and phospho-Fhit antisera, phospho-Fhit was not detected during this study of Y114. Thus, phosphorylation at Y114 is apparently not required for the proapoptotic activity of Fhit, but the Y114 residue in the unstructured loop is important in substrate-binding activity, and consequently essential for activation of Fhit apoptosis signals. Further investigation will be required to clarify the biological significance of phospho-Fhit, including the possibility that Src family proteins may downregulate Fhit activity by phosphorylating Y114, or that phosphorylated Fhit has a shorter half-life than the unphosphorylated form.

Nishizaki *et al*. (2004) reported synergistic tumor-suppressing effect by coexpression of Fhit and p53 and suggested that a Fhit–MDM2 complex interrupts p53–MDM2 interaction, resulting in stabilization of p53 protein and enhancement of p53 function in the regulation of cell cycle and apoptosis. However, as shown in this study, overexpression of wild-type Fhit induced caspase-dependent apoptosis in cells with (A549) or without (H1299) p53 expression (Ji *et al*., 1999; Trapasso *et al*., 2003). Although hUBC9, a SUMO-conjugating enzyme and M and S-phase cyclin regulator, has been proposed as a Fhit-binding molecule, it has not been clarified whether the Fhit–Ap_3A complex can bind to MDM2 or hUBC9 (Shi *et al*., 2000).

This is the first report showing inactivation of the PI3K-Akt-survivin pathway by wild-type Fhit, which is a novel molecular mechanism for Fhit-mediated apoptosis signaling. Akt, a member of the PI3K family, is activated in response to the generation of phosphatidylinositides and activated Akt in turn signals to a variety

Figure 4 Fhit protein modulates Akt activation and loss of Fhit expression enhances Akt phosphorylation. (**A**) Downregulation of Akt signaling by Ad-*FHIT*-wt but not Ad-*FHIT*-Y114F in H1299 cells. The cells were infected with Ad-*FHIT*-wt and Ad-*FHIT*-Y114F, respectively. Uninfected H1299 cells were also treated with PI3K inhibitor, LY294002 (20 μm) for 24 h, to illustrate that Akt and mTOR activation is controlled by the PI3K pathway. Ad-*GFP* infection did not alter phosphorylation levels of Akt, Src or mTOR (data not shown). (**B**) Specific suppression of endogenous Fhit by siRNA transfection in A549 cells. (**a**) Endogenous Fhit expression was effectively suppressed by *FHIT*-specific siRNA (5–50 nM) 24 h after transfection, but not by scrambled *FHIT* siRNA (25 nM). As control, siRNA against *GAPDH* mRNA was also used (data not shown). (**b**) Transfection of *FHIT* siRNA (25 nM) activated Akt protein. Significant upregulation of phosphorylated Akt was detected 24 h after infection but scrambled *FHIT* control did not alter the levels of phospho-Akt expression. (**C**) Immunohistochemical detection of Fhit, phospho-Akt (Ser473) and survivin in $Fhit^{+/+}$ and $Fhit^{-/-}$ mouse bronchial cells, and Fhit-deficient mouse tumor. (**a**, **b**, **c**) Expression of Fhit protein was detected in the cytoplasm of normal bronchial epithelium, whereas $Fhit^{-/-}$ bronchial cells and Fhit-deficient lung tumors did not exhibit Fhit expression (× 400). (**d**, **e**, **f**) Phosphorylated Akt expression was slightly upregulated in $Fhit^{-/-}$ mouse bronchus (× 400). The Fhit-deficient mouse lung tumor showed strong expression of phosphorylated Akt, and nuclear accumulation was also detected heterozygously (*inset*). (**g**, **h**, **i**) Survivin expression was not detected in normal bronchial cells, irrespective of presence or absence of *Fhit* allele (× 200). However, Fhit-deficient lung tumor showed high levels of survivin expression (× 200).

of key downstream molecules, including Bad, caspase-9, mTOR and GSK-3, the sum of which is to suppress cell death and to promote cell survival (Vivanco and Sawyers, 2002). Moreover, activation of PI3K-Akt signaling is required for upregulation of *survivin* expression as well as *STAT3* signal transducer (Papapetropoulos *et al*., 2000; Altieri, 2003; Fornaro *et al*., 2003; Dan *et al*., 2004). A requirement of the PI3K-Akt pathway for *survivin* expression has been shown in myeloma cells, in which apoptosis induced by a specific

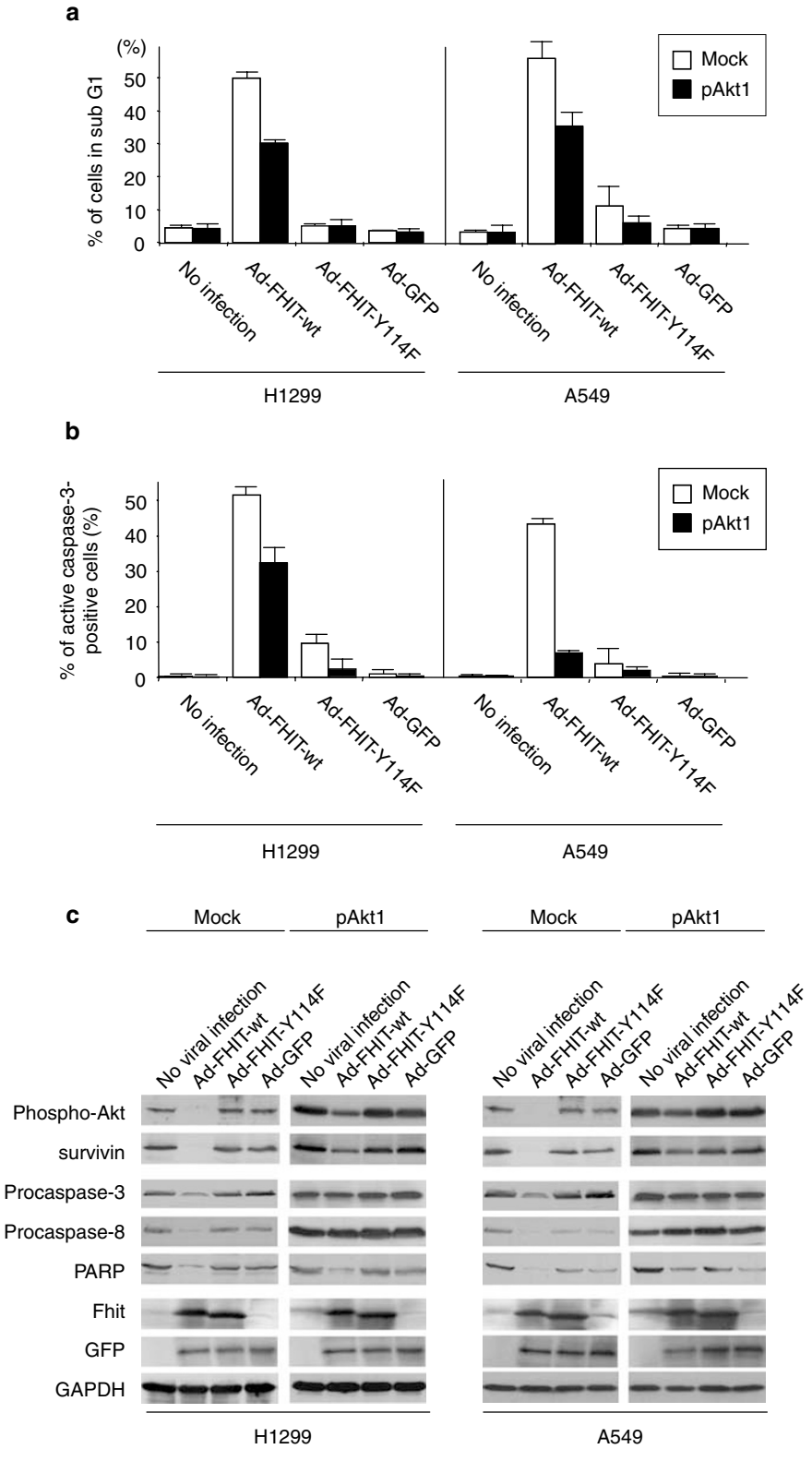

Akt inhibitor was counteracted by *survivin* expression via abrogation of NF-κB transcriptional activity (Mitsiades *et al*., 2002). Survivin is well known to interface both the cell-death machinery and mechanisms of cell cycle progression and microtubule stability (Dan *et al*., 2004). Survivin expression is undetectable in most normal adult tissues, but is overexpressed virtually in all human tumors. In the current study, despite the small structural difference between tyrosine and phenylalanine, neither downregulation of *survivin* expression nor inactivation of Akt was detected in Ad-*FHIT*-Y114F-infected cells. Although caspase-9 is one of the phosphorylation targets of Akt (Vivanco and Sawyers, 2002), we expected that caspase-9 would also be inactivated; however, expression of caspase-9 was undetectable in both H1299 and A549 cells (data not shown). Hence, this PI3K-Akt-survivin pathway plays an important role in the Fhit-induced apoptosis process. Although constitutively activated Akt decreased the percentage of the cells with subG1 DNA content and active caspase-3-positive cells induced by Ad-*FHIT*-wt, the tumor-suppressing activity of wild-type Fhit was not completely abrogated, suggesting the PI3K-Akt-survivin pathway is not the only signal pathway involved in Fhit-induced apoptosis. How might Fhit be involved in inactivation of Akt phosphorylation? Lu *et al*. (2003) reported that Src tyrosine kinase regulates the PI3K signaling cascade via alteration of the function of Pten, a negative regulator of the PI3K-Akt pathway; active Src kinase reduces the ability of Pten to dephosphorylate membrane phosphatidylinositides (PtdIns) by promoting Pten phosphorylation and degradation. One possibility for Fhit involvement is that overexpression of Fhit may suppress the tyrosine kinase activity of Src through interaction of Fhit and Src in the process of Fhit phosphorylation. The phosphatase activity of Pten might then be enhanced as a result of inactivation of Src, leading to inactivation of Akt. Further investigation will be required to define the details of the connection between Fhit and Akt signaling.

Exposure to genotoxic agents causes many human cancers and responses to such stresses are important defense mechanisms. We previously assessed the Atr-Chk1 pathway in response to mitomycin C, UVC and ionizing radiation in Fhit-positive and -negative cells and found that Fhit-negative cells are resistant to apoptosis induced by these genotoxic agents despite strong activation of the Atr-Chk1 pathway (Ottey *et al*., 2004; Hu *et al*., 2005). Moreover, as indicated previously, loss of Fhit expression is detected in cancers and premalignant lesions (Mao *et al*., 1997; Hao *et al*., 2000; Mori *et al*., 2000). Therefore, abnormalities in the *FHIT* gene or loss of Fhit expression has been considered an early or initiating event in multistep carcinogenesis. Upregulated basal levels of phosphorylated Akt and survivin in the Fhit$^{-/-}$ mouse bronchial cells may enhance their resistance against cell death signaling, and consequently accelerate accumulation of genetic alterations in oncogenes or tumor suppressor genes, contributing to the enhanced tumor susceptibility of Fhit knockout mice.

Materials and methods

Cell culture and gene transfection

H1299 (lacking Fhit and p53 expression) and A549 (expressing low levels of endogenous Fhit and wild-type p53) human lung cancer cell lines, obtained from the American Type Culture Collection (Manassas, VA, USA), were maintained in RPMI-1640 and D-MEM/F-12 medium, respectively. HEK293 cells maintained in D-MEM, were used for generation, amplification and titration of all recombinant adenoviruses (Ishii *et al*., 2001). The constitutively active *Akt1* construct (p*Akt1*) and control vector have been described (Pekarsky *et al*., 2000). Transfections into H1299 and A549 cells were carried out using Lipofectamine reagent (Invitrogen, Carlsbad, CA, USA) and stable clones were selected with 400 μg/ml of G418 sulfate. LY294002, an inhibitor of PI3K (Sigma-Aldrich St Louis, MO, USA), was dissolved in DMSO at a stock concentration of 10 mM and added to cell cultures at a final concentration of 20 μM.

Recombinant adenoviral vector construction and gene transduction

Mutant *FHIT* DNAs were designed to replace tyrosine with alanine (Fhit-Y114A), aspartic acid (Fhit-Y114D) and phenylalanine (Fhit-Y114F), as well as deletion mutant Fhit-Δ113–117. The wild-type and Y114 mutant *FHIT*-expressing adenoviruses were constructed as described previously (Ishii *et al*., 2001; Trapasso *et al*., 2003). Briefly, wild-type and mutant *FHIT* cDNAs were cloned into the transfer vector pAdenoVator-CMV5-GFP (Qbiogene, Carlsbad, CA, USA) upstream of internal ribosome entry sequence (IRES) and GFP. Linearized recombinant transfer vectors were recombined in BJ5183 *Escherechia coli* with the construct AdVator ΔE1/E3 containing a defective adenoviral genome. Resulting vectors were transfected into HEK293 cells to package viruses. Single viral plaques were isolated, expanded and checked for wild-type and mutant Fhit expression. The Ad-*GFP* was used as a nonspecific control for gene transfer (Qbiogene). The titer of each virus was determined by absorbance measurement, MOI test, and tissue culture infectious dose 50 ($TCID_{50}$)

Figure 5 Effects of constitutively active Akt on Fhit-mediated apoptosis signaling. SubG1 DNA content (**a**) and fraction of active caspase-3-positive cells (**b**) for Ad-*FHIT*-wt and Ad-*FHIT*-Y114F-infected human lung cancer cell lines (MOI 25). Akt expression vector, pAkt1 and empty vector control (mock) were transfected into H1299 and A549 lung cancer cells, respectively. Flow cytometric analysis of H1299 and A549 cells infected with wild-type and mutant *FHIT* (MOI 25) was performed 5 days after viral inoculation. For subG1 DNA content analysis, the cells were stained with PI. To detect active caspase-3-expressing cells, anti-cleaved caspase-3 mouse monoclonal antibody conjugated with PE was used. (**c**) Confirmation of suppression of Fhit-mediated apoptosis signaling by active Akt. H1299 and A549 cells were infected with wild-type and mutant *FHIT* viruses (MOI 25). Note the increased basal levels of phospho-Akt, caspase-3, caspase-8 and survivin expression in p*Akt1*-transfected cells. Although the effect of Ad-*FHIT*-wt on downregulation of caspase-3, caspase-8 and survivin was suppressed, there was no significant difference in PARP expression between p*Akt1* transfectant and control cells.

method. Adenoviral infection was performed with 5×10^5 cells, which had been cultured for 24 h prior to infection. Cells were incubated with adenoviral aliquots at a desired MOI for 4 h before addition of culture medium ($>25 \times$ volume of virus inoculum).

Cell viability and flow cytometric analysis

For cell viability tests, 5×10^5 cells were infected with individual adenoviruses (MOI 0–200), harvested, stained with trypan blue, and counted with the ViCell cell counter (Beckman Coulter, Fullerton, CA, USA). To analyse cellular DNA content, 5×10^5 cells were infected with individual recombinant adenovirus at an MOI of 25 and 5 days, cells were fixed in 70% methanol, treated with RNase A, and stained with propidium iodide (PI). For quantification of cells positive for active (cleaved) caspase-3, cells were washed, fixed, permeabilized and stained with phycoerythrin (PE)-conjugated monoclonal anti-active caspase-3 (BD Biosciences, San Jose, CA, USA). These analyses were performed with a FACS Calibur cytometer (BD Biosciences). Experiments were repeated thrice.

Western blot analysis

Samples were extracted in cell lysis buffer containing 50 mM Tris-HCl (pH 7.4), 125 mM NaCl, 0.1% Triton X-100, 5 mM EDTA, 1% (v/v) protease inhibitor cocktail (Sigma-Aldrich) and 1% (v/v) phosphatase inhibitor cocktail (Sigma-Aldrich). Fhit proteins (Brenner *et al*., 1997) and phosphorylated Fhit (Garrison *et al*., 2005) was purified, and values of K_m and k_{cat} for hydrolysis of Ap_3A were determined as described (Garrison *et al*., 2005). Total protein (30 μg) was separated on a 10 or 12% polyacrylamide gel (BioRad, Hercules, CA, USA) and transferred to a Hybond-C membrane (Amersham Biosciences, Piscataway, NJ, USA). Membranes were probed with antisera against Fhit (Fong *et al*., 2000), phospho-Fhit (Y114), caspase-3 (Santa Cruz biotechnology, Santa Cruz, CA, USA), and caspase-8 (Santa Cruz Biotechnology). Rabbit polyclonal phospho-Fhit (Y114) antiserum was custom made by Zymed laboratories (South San Francisco, CA, USA), against peptide: CRNDSI-pY-EELQ, affinity purified and absorbed against the unphosphorylated peptide (CRNDSI-Y-EELQ). Antisera against PARP, survivin, phospho-Akt (Ser473), phospho-Src (Tyr416), phospho-mTOR (Ser2448) were purchased from Cell Signaling (Beverly, MA, USA). As controls, GFP and GAPDH antibodies were used (Trapasso *et al*., 2003). After probing with appropriate secondary anti-rabbit or anti-mouse IgG conjugated to horseradish peroxidase, signals were detected by SuperSignal enhanced chemiluminescence substrate (Pierce, Rockford, IL, USA).

Immunofluorescence and immunohistochemistry

After infection with recombinant adenoviruses, cells in chamber slides were fixed with 4% formalin for 30 min, washed with phosphate-buffered saline (PBS) thrice, and incubated with blocking solution containing 1% bovine serum albumin in PBS. Cells were incubated with Fhit-specific antiserum for 2 h, rinsed with PBS, and incubated with Texas-Red conjugated anti-rabbit IgG in blocking buffer. Cells were rinsed with PBS thrice, mounted in 4′,6-diamidino-2-phenylindole (DAPI)-containing agent (Vector Laboratories, Burlingame, CA, USA), and examined using a fluorescence microscope. The levels of Fhit, phospho-Akt and survivin expression in lung tissue of $Fhit^{+/+}$ and $Fhit^{-/-}$ mice, as well as Fhit-deficient mouse lung adenocarcinoma tissues, were examined immunohistochemically. Antisera against Fhit, phospho-Akt and survivin used for Western blot analysis were also suitable for immunohistochemistry. A modified version of the immunoglobulin enzyme bridge technique was used (Semba *et al*., 2002). Sections were counterstained with hematoxylin.

Micorarray expression profiling

GeneChip Human genome U133A plus 2.0 arrays (Affymetrix, Santa Clara, CA, USA), containing probes for 14 500 characterized genes and expressed sequence tags, were used. Detailed protocols are available at http://cancergenetics.med.ohio-state.edu/microarray. Total RNA was purified from H1299 cells infected with Ad-*FHIT*-wt and Ad-*FHIT*-Y114F (MOI 25) for 48 and 72 h with TRIZOL reagent (Invitrogen). Integrity of individual RNAs was verified by denaturing agarose gel electrophoresis. *In vitro* transcription, oligonucleotide array hybridization and scanning were performed according to Affymetrix protocols. Briefly, double-stranded cDNA was synthesized from total RNA with SuperScript Choice System (Invitrogen), with a T7 RNA polymerase promoter site added to its 3′-end (Genset Corp., La Jolla, CA, USA). Biotinylated cRNAs were generated from cDNAs *in vitro* and amplified using the BioArray T7 RNA polymerase labeling kit (Enzo, Farmingdale, NY, USA). After purification of cRNAs by RNeasy mini kit (Qiagen, Hilden, Germany), 20 μg of cRNA was fragmented at 94°C for 35 min. Approximately 12.5 μg of fragmented cRNA was used in a 250-μl hybridization mixture containing herring sperm DNA (0.1 mg/ml; Promega, Madison, WI, USA), plus bacterial and phage cRNA controls (1.5 pM BioB, 5 pM BioC, 25 pM BioD and 100 pM Cre) to serve as internal controls for hybridization efficiency. Aliquots (200 μl) of the mixture were hybridized to arrays for 18 h at 45°C in a GeneChip Hybridization Oven 640 (Affymetrix). Each array was washed and stained with streptavidin–phycoerythrin (Invitrogen) and amplified with biotinylated anti-streptavidin antibody (Vector Laboratories) on the GeneChip Fluidics Station 400 (Affymetrix). Arrays were scanned with the GeneArray scanner (Agilent Technologies, Palo Alto, CA, USA) to obtain image and signal intensities.

Microarray data analysis

To minimize discrepancies due to variables such as sample preparation, hybridization conditions, staining or array lot, the raw expression data was scaled using the GeneChip Robust Multi-array analysis (GC-RMA) method, a modified method of Robust Multi-array Analysis (RMA), which uses nucleotide composition of probes. The GC-RMA method has better accuracy than Affymetrix Microarray Suite software ver. 5.0 (MAS 5.0) and some of the widely used alternatives, including RMA, dChip and PerfectMatch, to calculate expression values from probe level data. We used the significance analysis of microarrays (SAM) algorithm (Tusher *et al*., 2001) to detect differentially expressed transcripts in paired samples; that is Ad-*FHIT*-wt infected and Ad-*FHIT*-Y114F infected cultured cells at two times after infection. SAM computes a statistic (d_i) for each gene (i), measuring the strength of the relationship between gene expression and the response variable. It uses repeated permutations of the data to determine whether the expression of any gene is significantly related to the response. The cutoff for significance is determined by a tuning parameter Δ, chosen by the user based on the false discovery rate (FDR [$=0.2$]).

Quantitative real-time RT–PCR

Total RNAs were isolated from H1299 cells infected with Ad-*FHIT*-wt, Ad-*FHIT*-Y114F or Ad-*GFP*, respectively,

using the RNeasy Mini kit. Quantitative real-time RT–PCR analyses were performed using the iCycler multicolor real-time PCR detection system (Biorad) and the QuantiTect SYBR Green RT–PCR kit (Qiagen) as described elsewhere (Kato *et al*., 2004). The primer sets used in this study were; *survivin*-forward, 5′-AAGAACTGGCCCTTCTTGGA-3′; *survivin*-reverse, 5′-CAACCGGACGAATGCTTTT-3′; *GAPDH*-forward, 5′-GAAGGTGAAGGTCGGAGT-3′; *GAPDH*-reverse, 5′-GAAGATGGTGATGGGATTTC-3′. After an initial 30 min incubation at 50°C and 15 min denaturation at 95°C, the following cycling conditions (45 cycles) were used: denaturation at 94°C for 15 s, annealing at 60°C for 15 s and elongation at 72°C for 15 s. All experiments were performed in triplicate. Using *GAPDH* as a housekeeping gene, the expression levels of *survivin* mRNA were calculated as described (Junttila *et al*., 2003). The C_t values of triplicate RT–PCR reactions were averaged for each gene in each cDNA sample. For each tissue sample assayed, the average C_t value for the *survivin* gene was subtracted from the average C_t value of the *GAPDH* gene to obtain the ΔC_t value. The ΔC_t value of the reference sample was subtracted to obtain the $\Delta\Delta C_t$ value.

siRNA transfection

For RNA interference analyses, human *FHIT*-specific siRNA was designed and synthesized; sense, 5′-GGAAGGCUGGAG ACUUUGAtt-3′; antisense, 5′-UGAAAGUCUCCAGCCU UCCtt-3′ (Ambion, Austin, TX, USA). Control siRNAs for *FHIT* (scrambled: sense, 5′-UGACGGUUACGAGUAGG AGtt-3′; antisense, 5′-GUACGUACUCACGCUCUCAtt-3′) and for *GAPDH* (Ambion) were also used. All siRNA sequences were BLAST searched to confirm absence of homology to additional known human coding sequences. A549 cells, which express low levels of endogenous Fhit, were seeded in 24-well plates (1×10^5 cells/well). Next day siRNAs were added at final concentration (0–50 nM) in 500 μl D-MEM/F-12 without serum in the presence of siPORT Amine (Ambion). After siRNA transfection, cells were incubated in D-MEM/F-12, 10% fetal bovine serum. A549 cells treated only with siPORT Amine served as control. We confirmed high (>90%) transfectivity of these siRNAs labeled with Cy3 by Silencer siRNA Labeling Kit (Ambion).

Acknowledgements

This work was supported by USPHS grants from the National Cancer Institure, P01 CA77738 (K Huebner) and P01 CA78890 (CM Croce), State of Pennsylvania Tobacco Settlement funds, funds from the Breast Cancer Program of US DOD, BC043090 (D Iliopoulos) and NIH training Grant T32-HLO7780 (KA McCorkell).

We thank Dr Shuang-Yin Han, for assistance in preparation of the recombinant adenoviral vectors, Drs Chang-Gong Liu and Xiuping Liu for assistance with microarray analysis, Drs Masaki Mori and Koshi Mimori for contribution of the esophageal cancer cell lines and Angela Robinson for expert assistance with preparation of purified Fhit proteins.

References

Altieri DC. (2003). *Nat Rev Cancer* **3**: 46–54.
Ambrosini G, Adida C, Altieri DC. (1997). *Nat Med* **3**: 917–921.
Barnes LD, Garrison PN, Siprashvili Z, Guranowski A, Robinson AK, Ingram SW *et al*. (1996). *Biochemistry* **35**: 11529–11535.
Brenner C, Pace HC, Garrison PN, Robinson AK, Rosler A, Liu XH *et al*. (1997). *Protein Eng* **10**: 1461–1463.
Croce CM, Sozzi G, Huebner K. (1999). *J Clin Oncol* **17**: 1618–1624.
Dan HC, Jiang K, Coppola D, Hamilton A, Nicosia SV, Sebti SM *et al*. (2004). *Oncogene* **23**: 706–715.
Dumon KR, Ishii H, Fong LY, Zanesi N, Fidanza V, Mancini R *et al*. (2001b). *Proc Natl Acad Sci USA* **98**: 3346–3351.
Dumon KR, Ishii H, Vecchione A, Trapasso F, Baldassarre G, Chakrani F *et al*. (2001a). *Cancer Res* **61**: 4827–4836.
Fong LY, Fidanza V, Zanesi N, Lock LF, Siracusa LD, Mancini R *et al*. (2000). *Proc Natl Acad Sci USA* **97**: 4742–4747.
Fornaro M, Plescia J, Chheang S, Tallini G, Zhu Y-M, King M *et al*. (2003). *J Biol Chem* **50**: 50402–50411.
Fujishita T, Doi Y, Sonoshita M, Hiai H, Oshima M, Huebner K *et al*. (2004). *Br J Cancer* **91**: 1571–1574.
Garrison PN, Robinson A, Pekarsky Y, Croce CM, Barnes LD. (2005). *Biochemistry* **44**: 6286–6292.
Hao XP, Willis JE, Pretlow TG, Rao JS, MacLennan GT, Talbot IC *et al*. (2000). *Cancer Res* **60**: 18–21.
Hu B, Han SY, Wang X, Ottey M, Dicker A, Huebner K *et al*. (2005). *J Cell Physiol* **202**: 518–523.
Huebner K, Croce CM. (2003). *Br J Cancer* **88**: 1501–1506.
Huebner K, Garrison PN, Barnes LD, Croce CM. (1998). *Annu Rev Genet* **32**: 7–31.
Iliopoulos D, Guler G, Han SY, Johnston D, Druck T, McCorkell KA *et al*. (2005). *Oncogene* **24**: 1625–1633.
Ishii H, Dumon KR, Vecchione A, Trapasso F, Mimori K, Alder H *et al*. (2001). *Cancer Res* **61**: 1578–1584.
Ji L, Fang B, Yen N, Fong K, Minna FJ, Roth JA. (1999). *Cancer Res* **59**: 3333–3339.
Junttila TT, Laato M, Vahlberg T, Soderstrom KO, Visakorpi T, Isola J *et al*. (2003). *Clin Cancer Res* **9**: 5346–5357.
Kato H, Semba S, Miskad UA, Seo Y, Kasuga M, Yokozaki H. (2004). *Clin Cancer Res* **10**: 7318–7328.
Kuroki T, Trapasso F, Yendamuri S, Matsuyama A, Alder H, Mori M *et al*. (2003). *Cancer Res* **63**: 3724–3728.
Li F, Ambrosini G, Chu EY, Plescia J, Tognin S, Marchisio PC *et al*. (1998). *Nature* **396**: 580–584.
Lu Y, Yu Q, Liu JH, Zhang J, Wang H, Koul D *et al*. (2003). *J Biol Chem* **278**: 40057–40066.
Mao L, Lee JS, Kurie JM, Fan YH, Lippman SM, Lee JJ *et al*. (1997). *J Natl Cancer Inst* **89**: 857–862.
Mitsiades CS, Mitsiades N, Poulaki V, Schlossman R, Akiyama M, Chauhan D *et al*. (2002). *Oncogene* **21**: 5673–5683.
Mori M, Mimori K, Shiraishi T, Alder H, Inoue H, Tanaka Y *et al*. (2000). *Cancer Res* **60**: 1177–1182.
Nishizaki M, Sasaki J, Fang B, Atkinson EN, Minna JD, Roth JA *et al*. (2004). *Cancer Res* **64**: 5745–5752.
Ohta M, Inoue H, Cotticelli MG, Kastury K, Baffa R, Palazzo J *et al*. (1996). *Cell* **84**: 587–597.
Ottey M, Han SY, Druck T, Barnoski BL, McCorkell KA, Croce CM *et al*. (2004). *Br J Cancer* **91**: 1669–1677.
Pace HC, Garrison PN, Robinson AK, Barnes LD, Draganescu A, Rosler A *et al*. (1998). *Proc Natl Sci USA* **95**: 5484–5489.

Papapetropoulos A, Fultin D, Mahbouby K, Kalb RG, O'Connoy DS, Li F *et al*. (2000). *J Biol Chem* **275**: 9102–9105.
Pekarsky Y, Garrison PN, Palamarchuk A, Zanesi N, Aqeilan RI, Huebner K *et al*. (2004). *Proc Natl Acad Sci USA* **101**: 3775–3779.
Pekarsky Y, Koval A, Hallas C, Bichi R, Tresini M, Malstrom S *et al*. (2000). *Proc Natl Acad Sci USA* **97**: 3028–3033.
Roz L, Gramegna M, Ishii H, Croce CM, Sozzi G. (2002). *Proc Natl Acad Sci USA* **99**: 3615–3620.
Semba S, Itoh N, Ito M, Youssef EM, Harada M, Moriya T *et al*. (2002). *Clin Cancer Res* **8**: 3824–3831.
Sevignani C, Calin GA, Cesari R, Sarti M, Ishii H, Yendamuri S *et al*. (2003). *Cancer Res* **63**: 1183–1187.
Shi Y, Zou M, Farid NR, Paterson MC. (2000). *Biochem J* **352**: 443–448.
Siprashvili Z, Sozzi G, Barnes LD, McCue P, Robinson AK, Eryomin V *et al*. (1997). *Proc Natl Acad Sci USA* **94**: 13771–13776.
Sozzi G, Veronese ML, Negrini M, Baffa R, Cotticelli MG, Inoue H *et al*. (1996). *Cell* **85**: 17–26.
Trapasso F, Krakowiak A, Cesari R, Arkles J, Yendamuri S, Ishii H *et al*. (2003). *Proc Natl Acad Sci USA* **100**: 1592–1597.
Tusher VG, Tibshirani R, Chu G. (2001). *Proc Natl Acad Sci USA* **98**: 5116–5121.
Vivanco I, Sawyers CL. (2002). *Nat Rev Cancer* **2**: 489–501.
Zanesi N, Fidanza V, Fong LY, Mancini R, Druck T, Valtieri M *et al*. (2001). *Proc Natl Acad Sci USA* **98**: 10250–10255.

Supplementary information accompanies the paper on Oncogene website (http://www.nature.com/onc)